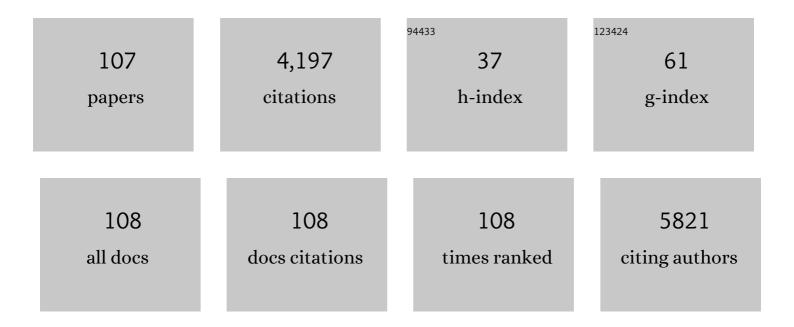
Xiaotian Li

List of Publications by Year in descending order

Source: https://exaly.com/author-pdf/3119928/publications.pdf Version: 2024-02-01



XIAOTIAN LI

#	Article	IF	CITATIONS
1	Activation engineering on metallic 1T-MoS2 by constructing In-plane heterostructure for efficient hydrogen generation. Applied Catalysis B: Environmental, 2022, 300, 120696.	20.2	60
2	Enhanced charge separation efficiency of sulfur-doped TiO2 nanorod arrays for an improved photoelectrochemical glucose sensing performance. Journal of Materials Science, 2022, 57, 1362-1372.	3.7	6
3	Ultrahigh Piezoelectric Performance through Synergistic Compositional and Microstructural Engineering. Advanced Science, 2022, 9, e2105715.	11.2	38
4	A Photoelectrochemical Platform Based on Polyaniline-Modified Titanium Dioxide Facet Heterostructure. ACS Applied Bio Materials, 2022, 5, 1297-1304.	4.6	1
5	Roles of hydroxyl and oxygen vacancy of CeO2·xH2O in Pd-catalyzed ethanol electro-oxidation. Science China Chemistry, 2022, 65, 877-884.	8.2	4
6	1T-MoS ₂ Nanosheets Coupled with CoS ₂ Nanoparticles: Electronic Modulation for Efficient Electrochemical Nitrogen Fixation. Inorganic Chemistry, 2022, 61, 7608-7616.	4.0	7
7	Unveiling the relationship between the multilayer structure of metallic MoS ₂ and the cycling performance for lithium ion batteries. Nanoscale, 2022, 14, 8621-8627.	5.6	9
8	Asymmetrically strained hcp rhodium sublattice stabilized by 1D covalent boron chains as an efficient electrocatalyst. Chemical Communications, 2021, 57, 5075-5078.	4.1	14
9	Electrochemical Fixation of Nitrogen by Promoting N ₂ Adsorption and N–N Triple Bond Cleavage on the CoS ₂ /MoS ₂ Nanocomposite. ACS Applied Materials & Interfaces, 2021, 13, 21474-21481.	8.0	39
10	PdCoNi alloy nanoparticles decorated, nitrogen-doped carbon nanotubes for highly active and durable oxygen reduction electrocatalysis. Chemical Engineering Journal, 2021, 411, 128527.	12.7	26
11	Synthesis of SnO2-nanoparticle-decorated SnSe nanosheets and their gas-sensing properties. AIP Advances, 2021, 11, .	1.3	3
12	Electrocaloric Performance of Multilayer Ceramic Chips: Effect of Geometric Structure Induced Internal Stress. ACS Applied Materials & Interfaces, 2021, 13, 38508-38516.	8.0	2
13	Realization of interstitial boron ordering and optimal near-surface electronic structure in Pd-B alloy electrocatalysts. Chemical Engineering Journal, 2021, 419, 129568.	12.7	23
14	Perovskite-SrTiO3/TiO2/PDA as photoelectrochemical glucose biosensor. Ceramics International, 2021, 47, 29807-29814.	4.8	10
15	Composition and strain engineered AgNbO ₃ -based multilayer capacitors for ultra-high energy storage capacity. Journal of Materials Chemistry A, 2021, 9, 9655-9664.	10.3	40
16	Ultrafine Cobaltâ€Doped Iron Disulfide Nanoparticles in Ordered Mesoporous Carbon for Efficient Hydrogen Evolution. ChemCatChem, 2020, 12, 788-794.	3.7	15
17	Self‣upported Mesoporous Iron Phosphide with High Active‣ite Density for Electrocatalytic Hydrogen Evolution in Acidic and Alkaline Media. ChemElectroChem, 2020, 7, 4943-4948.	3.4	10
18	Periodically ordered mesoporous iron phosphide for highly efficient electrochemical hydrogen evolution. Journal of Colloid and Interface Science, 2020, 569, 68-75.	9.4	11

Χιάοτιαν Li

#	Article	IF	CITATIONS
19	1T- and 2H-mixed phase MoS2 nanosheets coated on hollow mesoporous TiO2 nanospheres with enhanced photocatalytic activity. Journal of Colloid and Interface Science, 2020, 567, 10-17.	9.4	29
20	Enhanced Iridium Mass Activity of 6H-Phase, Ir-Based Perovskite with Nonprecious Incorporation for Acidic Oxygen Evolution Electrocatalysis. ACS Applied Materials & Interfaces, 2019, 11, 42006-42013.	8.0	48
21	Vertical nanosheet array of 1T phase MoS2 for efficient and stable hydrogen evolution. Applied Catalysis B: Environmental, 2019, 246, 296-302.	20.2	122
22	Ultra‧mall Molybdenum Carbide Nanoparticles inâ€situ Entrapped in Mesoporous Carbon Spheres as Efficient Catalysts for Hydrogen Evolution. ChemCatChem, 2019, 11, 2643-2648.	3.7	18
23	Three-dimensionally ordered macroporous FeP self-supported structure for high-efficiency hydrogen evolution reaction. International Journal of Hydrogen Energy, 2019, 44, 5854-5862.	7.1	16
24	Synthesis of hierarchically meso-macroporous TiO2/CdS heterojunction photocatalysts with excellent visible-light photocatalytic activity. Journal of Colloid and Interface Science, 2018, 512, 47-54.	9.4	77
25	Efficient oxygen evolution electrocatalysis in acid by a perovskite with face-sharing IrO6 octahedral dimers. Nature Communications, 2018, 9, 5236.	12.8	325
26	Threeâ€Dimensional Cathode Constructed through Confinedâ€Growth of FeP Nanocrystals in Ordered Mesoporous Carbon Film Coated on Carbon Cloth for Efficient Hydrogen Production. ChemCatChem, 2018, 10, 3441-3446.	3.7	7
27	Nano-netlike carbon fibers decorated with highly dispersed CoSe2 nanoparticles as efficient hydrogen evolution electrocatalysts. Journal of Alloys and Compounds, 2017, 702, 611-618.	5.5	20
28	Hypomethylation of tissue factor pathway inhibitor 2 in human placenta of preeclampsia. Thrombosis Research, 2017, 152, 7-13.	1.7	10
29	Rapid synthesis of rGO conjugated hierarchical NiCo ₂ O ₄ hollow mesoporous nanospheres with enhanced glucose sensitivity. Nanotechnology, 2017, 28, 025501.	2.6	29
30	In situ synthesis of concentric C@MoS2 core–shell nanospheres as anode for lithium ion battery. Journal of Materials Science, 2017, 52, 13183-13191.	3.7	22
31	3D NiO hollow sphere/reduced graphene oxide composite for high-performance glucose biosensor. Scientific Reports, 2017, 7, 5220.	3.3	132
32	Synthesis of CdS/m-TiO2 mesoporous spheres and their application in photocatalytic degradation of rhodamine B under visible light. Chemical Research in Chinese Universities, 2017, 33, 436-441.	2.6	11
33	Watermelon-like Rh x S y @C nanospheres: phase evolution and its influence on the electrocatalytic performance for oxygen reduction reaction. Journal of Materials Science, 2017, 52, 11402-11412.	3.7	5
34	Macroporous TiO ₂ encapsulated Au@Pd bimetal nanoparticles for the photocatalytic oxidation of alcohols in water under visible-light. RSC Advances, 2016, 6, 107233-107238.	3.6	8
35	Well-dispersed CoS ₂ nano-octahedra grown on a carbon fibre network as efficient electrocatalysts for hydrogen evolution reaction. Catalysis Science and Technology, 2016, 6, 4545-4553.	4.1	62
36	Hydrothermal synthesis of highly crystalline RuS2 nanoparticles as cathodic catalysts in the methanol fuel cell and hydrochloric acid electrolysis. Materials Research Bulletin, 2015, 65, 110-115.	5.2	29

XIAOTIAN LI

#	Article	IF	CITATIONS
37	A standing wave linear ultrasonic motor operating in in-plane expanding and bending modes. Review of Scientific Instruments, 2015, 86, 035002.	1.3	48
38	Heterostructures of Ag 3 PO 4 /TiO 2 mesoporous spheres with highly efficient visible light photocatalytic activity. Journal of Colloid and Interface Science, 2015, 450, 246-253.	9.4	55
39	Quantitative Proteomic Analysis of Serum from Pregnant Women Carrying a Fetus with Conotruncal Heart Defect Using Isobaric Tags for Relative and Absolute Quantitation (iTRAQ) Labeling. PLoS ONE, 2014, 9, e111645.	2.5	10
40	A two degrees-of-freedom piezoelectric single-crystal micromotor. Journal of Applied Physics, 2014, 116, .	2.5	40
41	One-pot synthesis of ordered mesoporous silver nanoparticle/carbon composites for catalytic reduction of 4-nitrophenol. Journal of Colloid and Interface Science, 2014, 423, 54-59.	9.4	80
42	Amino-functionalized magnetic mesoporous microspheres with good adsorption properties. Materials Research Bulletin, 2014, 49, 279-284.	5.2	52
43	Electrospun TiO ₂ nanofibers integrating space-separated magnetic nanoparticles and heterostructures for recoverable and efficient photocatalyst. Journal of Materials Chemistry A, 2014, 2, 12304-12310.	10.3	24
44	In situ synthesis of well crystallized rhodium sulfide/carbon composite nanospheres as catalyst for hydrochloric acid electrolysis. Journal of Materials Chemistry A, 2014, 2, 1484-1492.	10.3	14
45	Optical performance of mesostructured composite silica film loaded with organic dye. Applied Optics, 2014, 53, 291.	1.8	2
46	Hierarchical tubular structure constructed by mesoporous TiO2 nanosheets: Controlled synthesis and applications in photocatalysis and lithium ion batteries. Chemical Engineering Journal, 2013, 232, 356-363.	12.7	23
47	Electrospinning of magnetical bismuth ferrite nanofibers with photocatalytic activity. Ceramics International, 2013, 39, 3511-3518.	4.8	83
48	Spherical Rh17S15@C and Rh@C core–shell nanocomposites: Synthesis, growth mechanism and methanol tolerance in oxygen reduction reaction. Chemical Engineering Journal, 2013, 228, 45-53.	12.7	10
49	Magnetically separable Fe3O4@SiO2@TiO2-Ag microspheres with well-designed nanostructure and enhanced photocatalytic activity. Journal of Hazardous Materials, 2013, 262, 404-411.	12.4	132
50	Effect of large pore size of multifunctional mesoporous microsphere on removal of heavy metal ions. Journal of Hazardous Materials, 2013, 254-255, 157-165.	12.4	128
51	Phosphotungstic acid anchored to amino–functionalized core–shell magnetic mesoporous silica microspheres: A magnetically recoverable nanocomposite with enhanced photocatalytic activity. Journal of Colloid and Interface Science, 2013, 390, 70-77.	9.4	45
52	A high-temperature piezoelectric linear actuator operating in two orthogonal first bending modes. Applied Physics Letters, 2013, 102, .	3.3	21
53	A shear-bending mode high temperature piezoelectric actuator. Applied Physics Letters, 2012, 101, .	3.3	18
54	Preparation of magnetically recoverable Fe3O4@SiO2@meso-TiO2 nanocomposites with enhanced photocatalytic ability. Materials Research Bulletin, 2012, 47, 2396-2402.	5.2	64

XIAOTIAN LI

#	Article	IF	CITATIONS
55	Synthesis of Fe3O4@SiO2–Ag magnetic nanocomposite based on small-sized and highly dispersed silver nanoparticles for catalytic reduction of 4-nitrophenol. Journal of Colloid and Interface Science, 2012, 383, 96-102.	9.4	281
56	Facile encapsulation of monodispersed silver nanoparticles in mesoporous compounds. Chemical Engineering Journal, 2012, 195-196, 254-260.	12.7	24
57	Colossal low-frequency resonant magnetomechanical and magnetoelectric effects in a three-phase ferromagnetic/elastic/piezoelectric composite. Applied Physics Letters, 2012, 101, .	3.3	58
58	In situ auto-reduction of silver nanoparticles in mesoporous carbon with multifunctionalized surfaces. Journal of Materials Chemistry, 2012, 22, 13571.	6.7	40
59	Comprehensive study of mesoporous carbon functionalized with carboxylate groups and magnetic nanoparticles as a promising adsorbent. Journal of Colloid and Interface Science, 2012, 369, 366-372.	9.4	51
60	Study on a type of mesoporous silica humidity sensing material. Sensors and Actuators B: Chemical, 2012, 166-167, 658-664.	7.8	34
61	Effect of template-removing methods and modification to mesoporous blank silica and composited silica. Powder Technology, 2012, 219, 271-275.	4.2	5
62	Synthesis, Characterization, and Humidity Sensing Property of Mesoporous Cerium Oxide. Journal of Nanoengineering and Nanomanufacturing, 2012, 2, 41-45.	0.3	1
63	Humidity sensing properties of mesoporous iron oxide/silica composite prepared via hydrothermal process. Sensors and Actuators B: Chemical, 2011, 160, 334-340.	7.8	48
64	TiO2 supported on rod-like mesoporous silica SBA-15: Preparation, characterization and photocatalytic behaviour. Materials Research Bulletin, 2011, 46, 2317-2322.	5.2	19
65	Synthesis and characterization of structure optimized film doped with Rhodamine 6G. Journal of Sol-Gel Science and Technology, 2011, 59, 169-173.	2.4	0
66	Photoluminescence and laser properties of mesostructured SBA-15 monolith doped with coumarin 151. Journal of Sol-Gel Science and Technology, 2010, 54, 329-334.	2.4	4
67	Encapsulation of Coumarin 151 into the mesopores of modified rodlike SBA-15. Materials Research Bulletin, 2010, 45, 1-5.	5.2	4
68	Directâ€current and alternatingâ€current analysis of the humidityâ€sensing properties of nickel oxide doped polypyrrole encapsulated in mesoporous silica SBAâ€15. Journal of Applied Polymer Science, 2010, 115, 3474-3480.	2.6	30
69	Encapsulation of dye molecules into mesoporous polymer resin and mesoporous polymer-silica films by an evaporation-induced self-assembly method. Journal of Luminescence, 2010, 130, 512-515.	3.1	5
70	The humidity-sensitive property of MgO-SBA-15 composites in one-pot synthesis. Sensors and Actuators B: Chemical, 2010, 145, 386-393.	7.8	71
71	Synthesis and characterization of mesoporous indium oxide for humidity-sensing applications. Sensors and Actuators B: Chemical, 2010, 150, 442-448.	7.8	50
72	Preparation and humidity sensitive property of mesoporous ZnO–SiO2 composite. Sensors and Actuators B: Chemical, 2010, 149, 413-419.	7.8	74

Χιαότιαν Li

#	Article	IF	CITATIONS
73	H2S-sensing properties of Pt-doped mesoporous indium oxide. Applied Surface Science, 2010, 256, 5051-5055.	6.1	35
74	Ordered Arrays of Bead-Chain-like In ₂ O ₃ Nanorods and Their Enhanced Sensing Performance for Formaldehyde. Chemistry of Materials, 2010, 22, 3033-3042.	6.7	140
75	The study of photoluminescence properties of Rhodamine B encapsulated in mesoporous silica. Materials Chemistry and Physics, 2009, 118, 273-276.	4.0	48
76	Humidity sensitive property of Li-doped 3D periodic mesoporous silica SBA-16. Sensors and Actuators B: Chemical, 2009, 136, 392-398.	7.8	43
77	Study on humidity sensitive property of K2CO3-SBA-15 composites. Applied Surface Science, 2009, 256, 280-283.	6.1	18
78	Humidity-sensitive property of Fe2+ doped polypyrrole. Synthetic Metals, 2009, 159, 2469-2473.	3.9	37
79	Study on humidity sensing properties based on composite materials of Li-doped mesoporous silica A-SBA-15. Sensors and Actuators B: Chemical, 2008, 128, 482-487.	7.8	86
80	Synthesis and photoluminescent properties of mesoporous (MgO)x(ZnO)1â^'x materials. Materials Research Bulletin, 2008, 43, 601-610.	5.2	10
81	Mesoporous indium oxide synthesized via a nanocasting route. Materials Letters, 2008, 62, 3868-3871.	2.6	11
82	Ordered Mesoporous Copper Oxide with Crystalline Walls. Angewandte Chemie - International Edition, 2007, 46, 738-741.	13.8	124
83	Synthesis of cluster polyaniline nanorod via a binary oxidant system. Materials Science and Engineering C, 2007, 27, 695-699.	7.3	17
84	Synthesis and property of three novel organically templated layered cerium materials. Microporous and Mesoporous Materials, 2007, 101, 66-72.	4.4	6
85	Fluorescence of postgrafting Rhodamine B in the mesopores of rodlike SBA-15. Journal of Luminescence, 2007, 126, 723-727.	3.1	20
86	Effect of polymerization time on the humidity sensing properties of polypyrrole. Sensors and Actuators B: Chemical, 2007, 125, 114-119.	7.8	74
87	Humidity sensitive property of Li-doped mesoporous silica SBA-15. Sensors and Actuators B: Chemical, 2007, 127, 323-329.	7.8	82
88	Blue-shifting photoluminescence of Tris (8-hydroxyquinoline) aluminium encapsulated in the channel of functionalized mesoporous silica SBA-15. Materials Chemistry and Physics, 2006, 100, 128-131.	4.0	28
89	Synthesis of metallic nanotube arrays in porous anodic aluminum oxide template through electroless deposition. Materials Research Bulletin, 2006, 41, 1417-1423.	5.2	64
90	Synthesis of alumina nanowires and nanorods by anodic oxidation method. Materials Letters, 2006, 60, 2937-2940.	2.6	25

Xiaotian Li

#	Article	IF	CITATIONS
91	Humidity sensitivity of polypyrrole and polypyrrole/SBA-15 host–guest composite materials. Journal of Applied Polymer Science, 2006, 102, 3301-3305.	2.6	24
92	Low threshold amplified spontaneous emission based on coumarin 151 encapsulated in mesoporous SBA-15. Applied Physics Letters, 2006, 89, 231112.	3.3	15
93	Mesoporous silica tubes fabricated with human hair as template. Materials Chemistry and Physics, 2005, 91, 223-226.	4.0	4
94	Template synthesis of boron nitride nanotubes in mesoporous silica SBA-15. Materials Letters, 2005, 59, 925-928.	2.6	13
95	The fluorescence property of PNA encapsulated in the pores of oriented silicalite-1 film prepared on MSS. Materials Letters, 2005, 59, 2598-2600.	2.6	3
96	Crystal structures and magnetic properties of Fe–N thin films deposited by dc magnetron sputtering. Powder Diffraction, 2004, 19, 352-355.	0.2	7
97	Electroless deposition of open-end Cu nanotube arrays. Solid State Communications, 2004, 132, 841-844.	1.9	42
98	Synthesis and humidity sensitivity of conducting polyaniline in SBA-15. Journal of Applied Polymer Science, 2004, 93, 1597-1601.	2.6	52
99	Host–guest composite materials of LiCl/NaY with wide range of humidity sensitivity. Materials Letters, 2004, 58, 1535-1539.	2.6	26
100	The synthesis of offretite single crystals in the system containing pyrocatechol or Fâ^'. Materials Letters, 2001, 48, 1-7.	2.6	15
101	Synthesis of a High-Quality Host Material:  Zeolite MFI Giant Single Crystal from Monocrystalline Silicon Slice. Journal of Physical Chemistry B, 2001, 105, 12704-12708.	2.6	33
102	Size-controlled synthesis of silicalite-1 single crystals in the presence of benzene-1,2-diol. Microporous and Mesoporous Materials, 2000, 39, 117-123.	4.4	43
103	Light-emitting boron nitride nanoparticles encapsulated in zeolite ZSM-5. Microporous and Mesoporous Materials, 2000, 40, 263-269.	4.4	13
104	The role of pyrocatechol as a complex agent for silicon in the synthesis of large single crystals of silica-sodalite zeolite. Microporous and Mesoporous Materials, 1999, 33, 215-222.	4.4	22
105	Electrical conductivity of carbon fibers/ABS resin composites mixed with carbon blacks. Journal of Applied Polymer Science, 1996, 62, 2193-2199.	2.6	28
106	Energy-storage performance of NaNbO ₃ based multilayered capacitors. Journal of Materials Chemistry C, 0, , .	5.5	28
107	Crystal phase-selective synthesis of intermetallic palladium borides and phase-regulated (electro)catalytic properties. Catalysis Science and Technology, 0, , .	4.1	6